FUDMA Journal of Sciences (FJS)
ISSN online: 2616-1370
ISSN print: 2645 - 2944
Vol. 9 No. 12, December (Special Issue), 2025, pp 117 – 126
DOI: https://doi.org/10.33003/fjs-2025-0912-4226

THERMAL RADIATION AND CHEMICAL REACTION INFLUENCE ON MHD FLOW OF COUPLE STRESS FLUID PAST A VERTICAL PLATE

[1]Ayorinde Feyisayo, [1]Olajuwon, B. I., [1]Sogbetun, L. O., [1]Iyoko, M. O., [1]Raji, M. T., [1]Fagbemiro, O. and [2]Anyanwu, B. U.

[1]Department of Mathematics, Federal University of Agriculture, Abeokuta, Nigeria.
[2]Department of Mechanical Engineering, Federal University of Agriculture, Abeokuta, Nigeria.

*Corresponding authors' email: funaabfluidmechanicsresearch@gmail.com

ABSTRACT

The behavior of fluids which incorporate microstructural effects like couple stresses, is of notable interest due to their relevance in various engineering, industrial, and biomedical applications. In this study, a comprehensive numerical investigation into the combined effects of thermal radiation and chemical reaction on magnetohydrodynamic (MHD) flow of a couple stress fluid past a vertical plate is presented. Through the application of similarity transformations, the governing equations are reduced to nonlinear ordinary differential equations. The transformed equations are solved using the BVP4C method in MATLAB, which is based on the Lobatto IIIa collocation technique, ensuring accurate and efficient numerical computations. The impact of the various parameters on velocity, temperature, and concentration within the boundary layer are illustrated graphically. Furthermore, numerical results for the local Nusselt number and Sherwood number are presented in tabular form to highlight the sensitivity of thermal and mass transport to these physical effects. The results reveal that an increase in the couple stress parameter significantly alters the fluid motion, reducing velocity near the plate and enhancing temperature and concentration profiles. Thermal radiation and magnetic field effects increase the temperature while reducing velocity, indicating energy retention and resistive electromagnetic forces. Chemical reaction reduce concentration due to reactant consumption, while Soret and Dufour effects display a complex interplay between thermal and concentration gradients. These findings not only provide physical insight into the flow behavior under multiple interactive influences but also offer valuable guidance for controlling heat and mass transfer in MHD systems involving complex non-Newtonian fluids.

Keywords: BVP4C method, Chemical reaction, Couple stress fluid, Magnetohydrodynamics, Thermal radiation

INTRODUCTION

The theory of couple stress fluid originally developed by Stokes (1966), defines the rotational field in terms of the velocity field for setting up the constitutive relationship between the stress and strain rate. The micro-continuum theory of Stokes is the simplest generalization of the classical theory of fluids, which allows for polar effects such as the presence of couple stresses, body couples and a non-symmetric stress tensor. Couple stress fluid theory has indeed been employed to study a number of flow situations such as; low concentration suspension liquid crystals and blood flow. The theory may also be applied to explain the flow of colloidal solutions, fluids with additives and other solutions. In recent years, scientists have shown their interest in non-Newtonian fluids because of their applications in many natural, industrial and technological problems. The slow steady flow of couple stress fluids external to axisymmetric bodies has been studied by Ramkissoon (1978), who derived an expression for drag experienced by a sphere using a stream function approach, Ramalakshmi and Shukla (2021) conducted a rigorous analysis of the creeping flow of couple stress fluid from a sphere containing a solid core. The drag coefficient was analytically computed and showed that as couple stress parameter (inverse length dependence) increases the velocity, drag force and the pressure decreases. However, it was also noted that with increasing couple stress viscosity coefficient, the drag also increased. Furthermore, they found that with greater couple stress parameter and radius ratio there was a decrement in pressure. Aparna et al. (2007) and Aparna et al. (2008) computed the oscillatory and uniform steady flows, respectively of a couple stress fluid through a permeable sphere using the Darcy-Brinkman model. Farooq et al. (2018) presented a peristaltic modeling of couple stress fluid by embedding nanoparticles on coaxial channel. In this, they examined techniques for treatment of disastrous diseases like tumor and rheumatoid arthritis by injecting nanoparticles of gold in veins. In suggested model, the high atomic number permits nanoparticles of gold to get more heat to deliver medicine in effected area and erodes malign cells and tissues. Ahmed et al. (2014) considered the effect of heat transport by the influence of free convection flow of magnetohydrodynamic couple stress fluid due to an inclined rotating surface. Hassan et al. (2020) examined a model of couple stress with hydrodynamic to inspect the impact of heat generation and viscosity parameter in convective cooling wall. Srinivasacharya et al. (2012) explored the couple stress fluid f low. They originate that the couple stress parameter diminishes the fluid velocity and temperature. Ramzan et al. (2013) deliberated the couple stress fluid flow over extending sheet. It is found that velocity profiles along both directions are declined with the escalation in couple stress parameter. Also the fluid temperature escalated with viscous dissipation effect. Hayat et al. (2013) determined the heat transmission rate in the couple stress flow over extending surface and originate that the heat transfer intensifies with the rising estimations of the couple stress. Over an extending sheet, the couple stress fluid flow was determined by Turkyilmazoglu (2014). It is concluded that over a stretching sheet the couple stress gives double solution while over shrinking sheet it gives triple solution. The unsteady couple stress fluid flow was determined by Awad et al. (2016). Here, the fluid velocity and temperature decline with heightened couple stress. Sreenadh et al. (2011) examined the fluid flow with couple stress impact. Hayat et al. (2012) analyzed the mass transfer in

couple stress fluid with chemical reaction. Khan et al. (2014) scrutinized the incompressible and unsteady couple stress fluid flow considering three dimensional cylindrical polar coordinate systems

In recent times, the researchers have got interest in megnetohydrodynamic (MHD) owing to plentiful applications in industrial, engineering, and medical devices. Rudolf et al. (2014) briefly reviewed the properties of magnetic field in the universe. The MHD nanofluid flow with chemical reaction was deliberated by Hayat et al. (2016). The fluid flow velocity is reduced with higher estimation of magnetic field, and temperature escalated with chemical reactions and Dufour influences. The heat transmission in the flow of MHD nano fluid over unsteady extending sheet was observed by Lin et al. (2015). The fluid flow velocity is reduced with heightens in magnetic field while the temperature of the fluid escalated. The heat transfer in the flow of MHD incompressible second-grade nanofluid was deliberated by Ramesh et al. (2015). The MHD nanofluid flow in a symmetric channel was probed by Reddy et al. (2015). The elementary study of micropolar fluid was introduced by Eringen (1966). Bég et al. (2011) presented the applications of micropolar fluid flow. Khan et al. (2018) determined the radiation and inertial coefficient influences on the flow of nanofluid. The higher inertial coefficient, porosity parameter, and coupling parameter reduce the fluid velocity and the temperature heightens with the escalation in thermal radiation. Dawar et al. (2019) deliberated the unsteady MHD nanofluid with viscous dissipation effect. Here, the authors originate that the fluid flow velocity reduces with escalation in magnetic field and the fluid flow temperature reduces with viscous dissipation impacts. Kumam et al. (2019) probed the MHD Casson nanofluid flow. Shah et al. (2019a) deliberated the flow of MHD thin film fluid with radiation impact. The MHD Casson nanofluid flow in a cylindrical tube was considered by Ali et al. (2017). The MHD nanofluid flow with magnetic and electric fields, and Hall impacts was determined by Shah et al. (2019b). Kumar et al. (2019) investigated the MHD nanofluid with magnetic and heat sink/source impacts. Temple et al. (2015) scrutinized the nanoparticles of ferromagnetic for their size and magnetic properties. Ellahi et al. (2018) examined the MHD nanofluid flow with thermal conductivity. Some related articles to this work are Uddin et al. (2013) and Bhatti et al. (2018). Motivated from above assumptions, we investigate impact of thermal radiation and chemical reaction of mhd flow of couple stress fluid over vertical plate. The governing equations of above mentioned model are occurred in PDEs form and then these PDEs are transformed by applying transformations into ODEs. The numerical solution is analyzed by using a well-defined numerical approach "BVP4C method in matlab based on the Lobatto-IIIa collocation formula and the graphical outcomes of key parameters on different profiles are displayed.

Mathematical Formulation

Consider a two-dimensional flow of a couple stress fluid past a vertical plate in the presence of thermal radiation and chemical reaction. The coordinate system is such that x-axis is along the vertical plate and y-axis normal to the plate. The plate is maintained at a uniform wall temperature (T_w).and concentration (C_w). These values are assumed to be greater than the ambient temperature (T_∞) and concentration (C_∞) at any arbitrary reference point in the medium (inside the boundary layer). In addition, the Soret and Dufour effects are considered (Dougall 1982) The flow configuration and the coordinates system are shown in Figure 1.

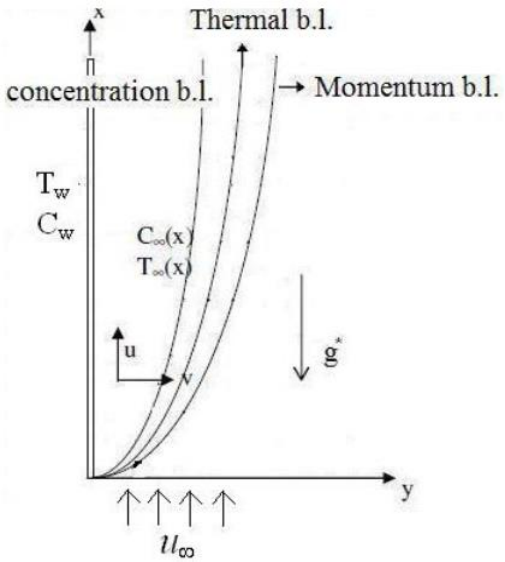

Figure 1: Physical model and coordinate system

The governing equation of the flow, heat and mass transfer are given below

$$\frac{\partial u}{\partial x}+\frac{\partial u}{\partial y}=0 \quad (1)$$

$$u\frac{\partial u}{\partial x}+v\frac{\partial u}{\partial y}=\upsilon\frac{\partial^2 u}{\partial y^2}-\frac{\eta_1}{\rho}\frac{\partial^4 u}{\partial y^4}+g[\beta_T(T-T_\infty)+\beta_C(C-C_\infty)]-\frac{\sigma\beta^2 u}{\rho} \quad (2)$$

$$u\frac{\partial T}{\partial x}+v\frac{\partial T}{\partial y}=\alpha\frac{\partial^2 T}{\partial y^2}+\frac{DK_T}{\rho c_p}\frac{\partial^2 C}{\partial y^2}-\frac{1}{\rho c_p}\frac{\partial q_r}{\partial y} \quad (3)$$

$$u\frac{\partial C}{\partial x}+v\frac{\partial C}{\partial y}=D\frac{\partial^2 C}{\partial y^2}+\frac{DK_T}{T_m}\frac{\partial^2 T}{\partial y^2}-R_C(C-C_\infty) \quad (4)$$

Where u, v are the velocity components in the x and y directions respectively, μ is the coefficient of viscosity thermal, g is the acceleration due to gravity, ρ is the density, β_T is the coefficient of thermal expansion $\beta_C$is the coefficient of solutal expansion,

α is the thermal diffusivity, D is the mass diffusivity , $C_p$is the specific heat capacity, $C_\infty$is the ambient concentration, $T_m$is the mean fluid temperature , $K_T$is the thermal diffusion ratio and η_1 is the couple stress fluid term. The last terms on the right-hand side of the momentum equation (2), energy equation (3) and concentration equation (4) signifies the magnetic effect, thermal radiation effect, and chemical reaction effect

The boundary conditions are

$u = 0, v = 0, C = C_w, V_x = U_y,$ at $y = 0$ (5)

$u \to u_\infty, T \to T_\infty, C \to C_\infty,$ as $y \to 0$ (6)

The subscript $w$and ∞ indicate the condition at the wall and at the outer edge of the boundary layer respectively. In view of the continuity equation (1), we introduce the stream function by

$$u = \frac{\partial \psi}{\partial y}, v = -\frac{\partial \psi}{\partial y} \quad (7)$$

Substituting Equation (7) in Equations (2) - (4) and then using the following local similarity transformations below

$$\eta = \frac{y}{x} Re_x^{\frac{1}{2}}, u = u_\infty f'(\eta), v = -\frac{1}{2}\sqrt{\frac{u_x v}{x}}\left[f(\eta) - \eta f'(\eta)\right] \quad (8)$$

$$\theta(\eta) = \frac{T - T_\infty}{T_w - T_\infty}, \varphi(\eta) = \frac{C - C_\infty}{C_w - C_\infty}$$

After the similarity transformation of equation (1) - (4) and boundary conditions (5) and (6), the following nonlinear system differential equation (9) – (11) are obtained:

$$f'''(\eta) + \frac{1}{2} f f'' + g_s\theta + g_c\varphi - Caf^v(\eta) - mf'(\eta) = 0 \quad (9)$$

$$\theta''(\eta) + \frac{1}{2} P_r f(\eta)\theta'(\eta) + D_f P_r \varphi''(\eta) + \frac{4}{3} R_a P_r \theta''(\eta) = 0 \quad (10)$$

$$\varphi''(\eta) + \frac{1}{2} S_c f(\eta)\varphi'(\eta) + S_c S_r \varphi''(\eta) - CrS_c = 0 \quad (11)$$

Boundary conditions (5) and (6) in terms of f, θ and φ becomes

$$\left.\begin{array}{l} f(0) = 0 f'(0) = 0 f''(0) = 0\theta(0) = 1\varphi(0) = 1 \\ f'(\infty) = 1 f''(\infty) = 0\theta(\infty) = 0\varphi(\infty) = 0 \end{array}\right\} \quad (12)$$

Where primes denote differentiation with respect to η, chemical reaction parameter is $Cr = \frac{R_C}{u_\infty}$, $Sc = \frac{\upsilon}{D}$ is the Schmidt number, $Pr = \frac{\upsilon}{\alpha}$ is the Prandtl number, $Re_x = \frac{u_\infty x}{\upsilon}$ is the local Reynolds number, $S_r = \frac{DK_T(T_w - T_\infty)}{\upsilon T_m (C_w - C_\infty)}$ is the Soret number, $D_f = \frac{DK_T(C_w - C_\infty)}{\upsilon C_S c_p (T_w - T_\infty)}$ is the Dufour number,

$Gr_x = \frac{g\beta_T(T_w - T_\infty)x^3}{\upsilon^2}$ is the local temperature Grashof number, $Gc_x = \frac{g\beta_C(C_w - C_\infty)x^3}{\upsilon^2}$ is the local mass Grashof number, $C_\alpha = \frac{\eta_1}{\mu x^2} Re_x$ is the local couple stress parameter, $g_s = \frac{Gr_x}{Re_x^2}$ is the temperature buoyancy parameter and $g_c = \frac{Gc_x}{Re_x^2}$ is the mass buoyancy parameter, $M = \frac{\sigma {\beta_0}^2}{u_\infty \rho}$ is the Magnetic parameter , $\alpha = \frac{k}{\rho c_p}$ is the thermal diffusivity number, $\upsilon = \frac{\mu}{\rho}$ is the kinematic viscosity, $Rd = \frac{4\sigma^* T^4}{kk}$ is the radiation parameter, local Nusselt number is $Nu_x = \frac{xq_w}{k(T_w - T_\infty)}$, and local Sherwood number is$Sh_x = \frac{xq_w}{D(C_w - C_\infty)}$

Method of Solution

The dimensionless governing equations (9) – (11) alongside their boundary conditions in equation (12) are solved respectively by the BVP4C method in MATLAB based on the Lobatto-IIIa collocation formula used for numerical computation.

From equations (9) - (11) we have equations (13) - (15)

$$f^v = \frac{1}{C_a}\left(f''' + \frac{1}{2} f f'' + g_s\theta + g_c\varphi - Mf'\right) \quad (13)$$

$$\theta'' = -\left(\frac{3Pr}{3+4R_d - 3\,Pr\,D_f S_c S_r}() \left(\frac{1}{2} f\theta' + D_f\left(S_c C_r - \frac{1}{2} S_c f\varphi'\right)\right)\right) \quad (14)$$

$$\varphi'' = S_c C_r - \frac{1}{2} S_c f\varphi' + \left(\frac{3\,Pr\,S_c S_r}{3+4R_d - 3\,Pr\,D_f S_c S_r}\right)\left(\frac{1}{2} f\theta' + D_f\left(S_c C_r - \frac{1}{2} S_c f\varphi'\right)\right) \quad (15)$$

$$f = y_1 \quad f' = y_2 \quad f'' = y_3 \quad f''' = y_4 \quad f^{iv} = y_5 \quad (16)$$

$$\theta = y_6 \quad \theta' = y_7 \grave{} \quad \theta'' = y_7' \quad \varphi = y_8 \quad \varphi' = y_9 \quad (17)$$

By applying transformation in equations (13) - (17) to equations (9) - (12), we have the system of first order differential equations in (18) – (20) and the new boundary conditions in equation (21)

$$y_5' = \frac{1}{C_a}\left(y_4 + \frac{1}{2} y_1 y_3 + g_s y_6 + g_c y_8 - My_2\right) \quad (18)$$

$$y_7' = -\left(\frac{3Pr}{3+4R_d - 3\,Pr\,D_f S_c S_r}() \left(\frac{1}{2} y_1 y_7 + D_f\left(S_c C_r - \frac{1}{2} S_c y_1 y_9\right)\right)\right) \quad (19)$$

$$y_9' = S_c C_r - \frac{1}{2} S_c y_1 y_9 + \left(\frac{3\,Pr\,S_c S_r}{3+4R_d - 3\,Pr\,D_f S_c S_r}\right)\left(\frac{1}{2} y_1 y_7 + D_f\left(S_c C_r - \frac{1}{2} S_c y_1 y_9\right)\right) \quad (20)$$

$$\left.\begin{array}{l} y_1(0) = 0 y_2(0) = 0 y_3(0) = 0 y_6(0) = 1 y_8(0) = 1 \\ y_2(\infty) = 1 y_3(\infty) = 0 y_6(\infty) = 0 y_8(\infty) = 0 \end{array}\right\} \quad (21)$$

RESULTS AND DISCUSSION

Table1: Comparison of Results when $Pr = 0.71, g_s = 1.00, g_c = 0.10, C_\alpha = 1.00, Sc = 0.22, M = Rd = Cr = 0$

D_f	S_r	Srinivasacharya and Kaladhar (2012)		Present Results	
		Nu_x	Sh_x	Nu_x	Sh_x
2.00	0.03	0.2610	0.2256	0.2610	0.2256
1.00	0.06	0.2868	0.2220	0.2868	0.2220
0.60	0.10	0.2966	0.2198	0.2966	0.2198
0.40	0.15	0.3014	0.2179	0.3014	0.2179
0.15	0.40	0.3074	0.2101	0.3074	0.2101
0.10	0.60	0.3087	0.2043	0.3087	0.2043
0.06	1.00	0.3098	0.1928	0.3098	0.1928
0.03	2.00	0.3111	0.1642	0.3111	0.1642

Table 2: Numerical Values of Nusselt Number(Nu_x)and Sherwood Number (Sh_x)

D_f	S_r	Pr	Rd	Sc	Cr	C_α	M	g_S	g_c	Nu_x	Sh_x
0.05	0.03	0.71	0.4	0.22	0.05	0.5	0.2	1.00	0.10	0.2709	0.2386
1.00										0.2473	0.2409
2.00										0.2211	0.2433
0.05	1.00									0.2716	0.2190
	2.00									0.2723	0.1985
	0.03	2.00								0.3583	0.2299
		3.00								0.3984	0.2267
		0.71	0.6							0.2598	0.2398
			0.8							0.2508	0.2409
			0.4	0.4						0.2694	0.2866
				0.6						0.2681	0.3307
				0.22	0.5					0.2673	0.3740
					1.0					0.2643	0.4917
					0.05	1.00				0.2586	0.2323
						2.00				0.2452	0.2256
						0.50	0.50			0.2490	0.2269
							1.00			0.2265	0.2157
							0.20	2.00		0.3015	0.2551
								3.00		0.3233	0.2673
								1.00	0.50	0.2876	0.2475
									1.00	0.3050	0.2572

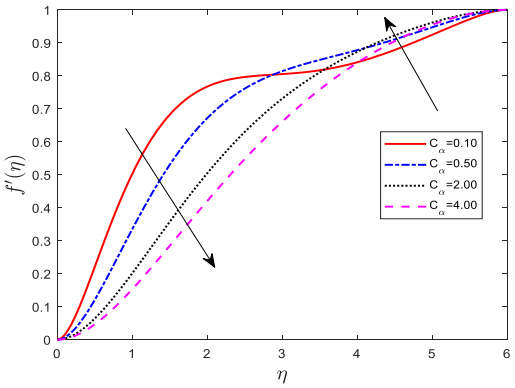

Figure 2: Effect of Couple stress parameter (C_α) on velocity $f'(\eta)$

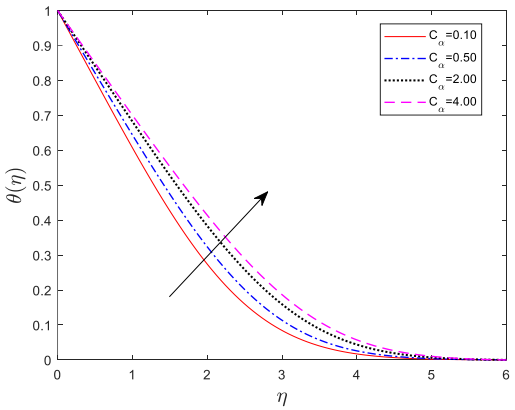

Figure 3: Effect of Couple stress parameter (C_α) on temperature$\theta(\eta)$

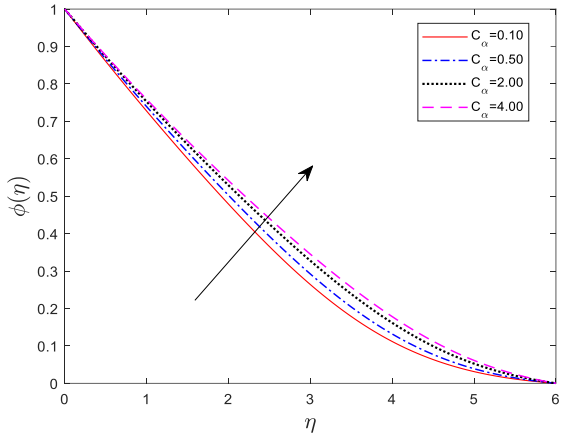

Figure 4: Effect of Couple stress parameter (C_α) on concentration (φ_η)

Figure 2, 3 and 4 show the impact of the couple stress parameter (C_α) on the velocity $f'(\eta)$, temperature $\theta(\eta)$ and concentration $\varphi(\eta)$ respectively. An increment in the value of Couple stress parameter is observed to decline the velocity profile at the wall plate and increased speedily far from wall. While on temperature and concentration an enhancement is noticed. This contributes to more dynamic interactions within the fluid, enhancing transport the process.

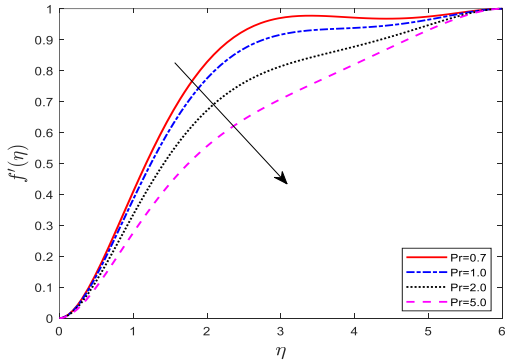

Figure 5: Effect of Prandtl (Pr) on velocity $f'(\eta)$

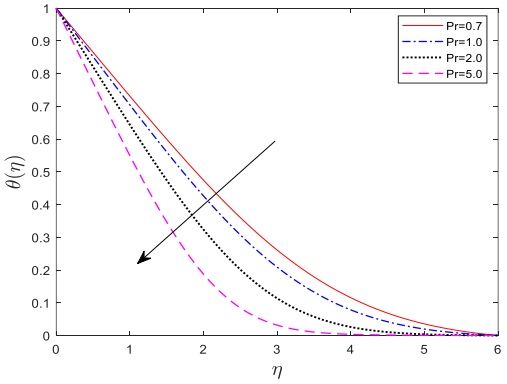

Figure 6: Effect of Prandtl (Pr) on temperature $\theta(\eta)$

Figure 5 and 6 illustrates the significance of Prandtl number (Pr) on Velocity$f'(\eta)$ and Temperature $\theta(\eta)$. Decrease in velocity and temperature is noticeable due to increase in Prandtl number. The result is because fluid with higher Prandtl number possesses higher viscosities which led to the decrease in thickness of the hydrodynamic and thermal boundary layers.

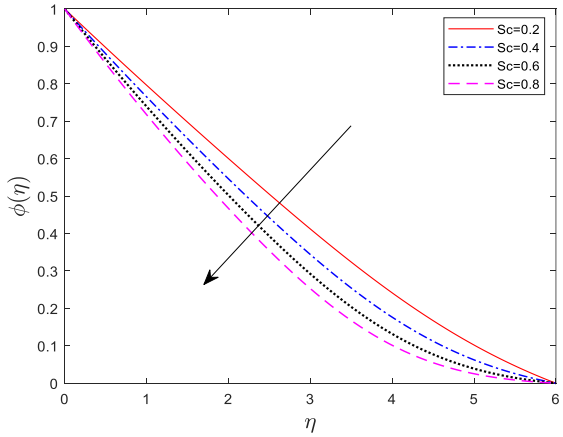

Figure 7: Effect of Shmidt (S_c) on concentration$\varphi_{(\eta)}$

Figure 7 shows the effect of Schmidt (Sc) number on the concentration profile. An Increase in Schmidt number is observed to reduce the concentration, the reason is that, when the Schmidt number is high, the solute concentration tends to remain closer to its source leading to less spreading and slower mixing throughout the fluid.

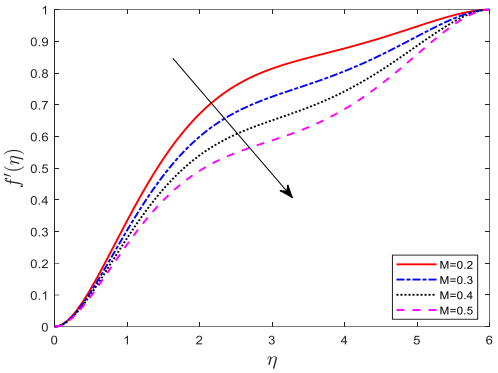

Figure 8: Effect of magnetic parameter (M) on velocity $f'(\eta)$

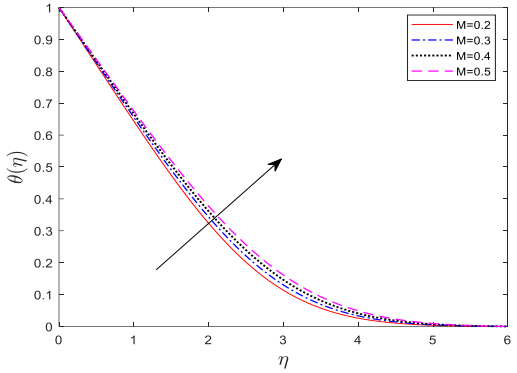

Figure 9: Effect of magnetic parameter (M) on temperature $\theta(\eta)$

Figure 8 and 9 show the impact of magnetic parameter (M) on velocity $f'(\eta)$ and temperature$\theta(\eta)$. It is observed that an increase in magnetic parameter, diminished the velocity and increased the temperature spontaneously This is because of the Lorentz force (resistive force) exerted, which caused the velocity to be reduced and enhanced the thermal retention, thereby making the temperature to increase vigorously.

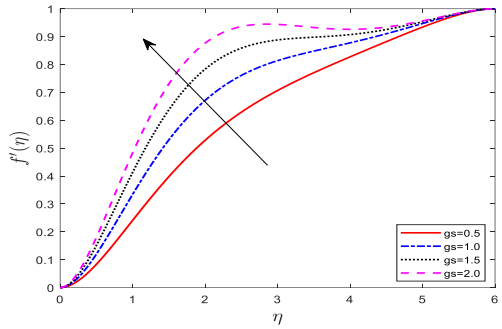

Figure 10: Effect of temperature buoyancy (g_s) on velocity$f'(\eta)$

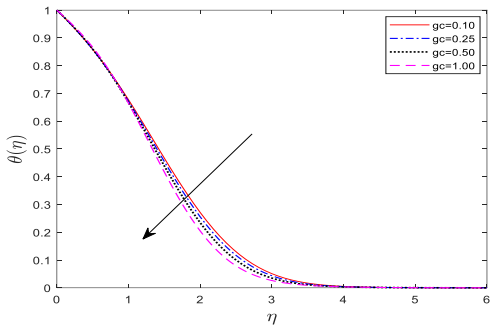

Figure 11: Effect of temperature buoyancy (g_s) on temperature $\theta(\eta)$

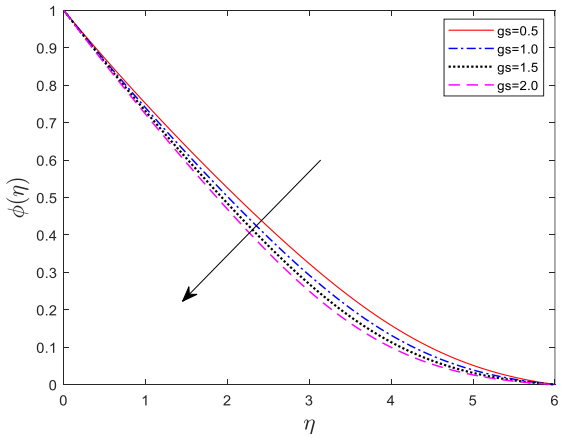

Figure 12: Effect of temperature buoyancy (g_s) on concentration $\varphi(\eta)$

Figure 10 to 12 illustrates the effect of temperature buoyance parameter (g_s) on velocity$f'(\eta)$ temperature $\theta(\eta)$ and concentration $\varphi(\eta)$ respectively. It is noticed that an increment in temperature buoyance enhanced the velocity but reduced the temperature and the concentration, due to the fact that intensified buoyancy forces promote more vigorous fluid motion as heated fluid becomes less dense and rises. This ultimately causes the concentration of the fluid to drop. Whereas the reduction in temperature occurred because the faster-moving fluid has less time to exchange heat with its surroundings resulting in lower thermal gradient.

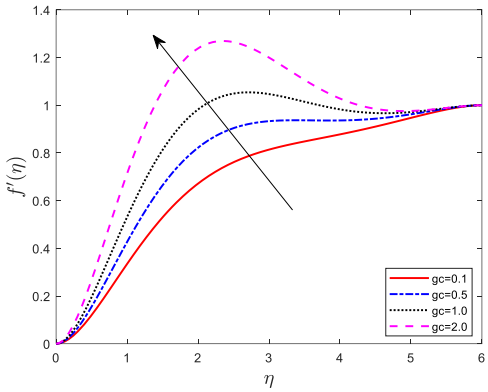

Figure 13: Effect of mass buoyancy (g_c) on velocity$f'(\eta)$

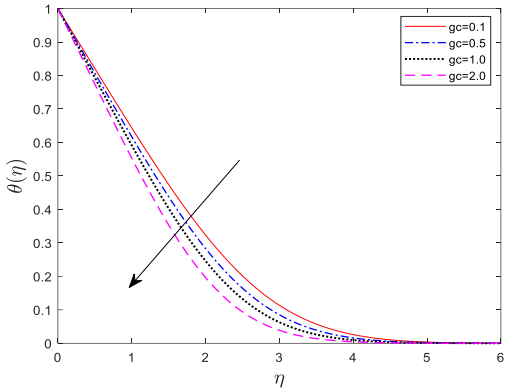

Figure 14: Effect of mass buoyancy (g_c) on temperature $\theta(\eta)$

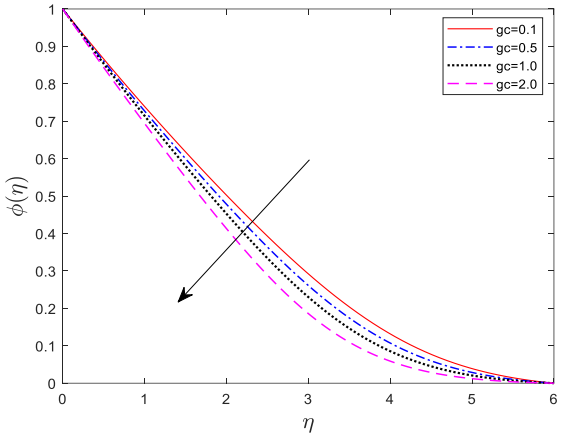

Figure 15: Effect of mass buoyancy (g_c) on concentration $\varphi(\eta)$

Figure 13, 14 and 15 show the impact of mass buoyance parameter (g_c) on velocity$f'(\eta)$, temperature $\theta(\eta)$ and concentration $\varphi(\eta)$ respectively. It is seen that an increase in mass buoyance parameter caused Velocity profile to increase at the wall plate and decreased towards a distance far to the wall, because of boundary layer development i.e. Near the wall the fluid adheres to the surface due to the no-slip. While Temperature profile and Concentration profile, decreased spontaneously due to diminished viscous effects and increased heat transfer efficiency

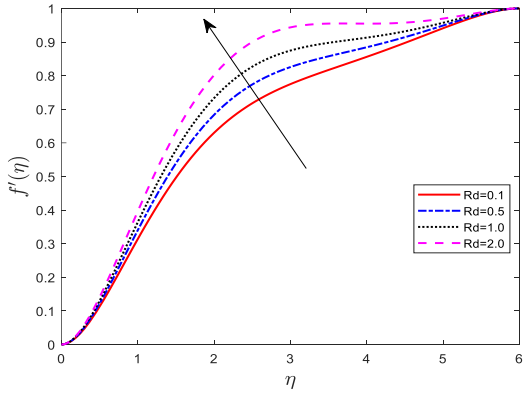

Figure 16: Effect of radiation parameter (Rd) on velocity$f'(\eta)$

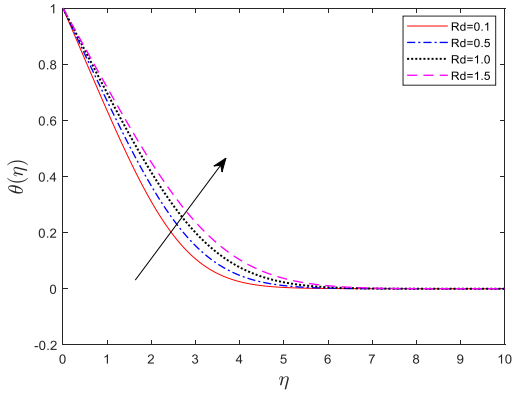

Figure17: Effect of radiation parameter (Rd) on temperature $\theta(\eta)$

Figure, 16 and 17 explain the effect of Radiation parameter(Rd)on velocity$f'(\eta)$ and temperature$\theta(\eta)$. It is observed that increase in thermal radiation parameter increased the velocity and temperature profile, because as the radiation parameter rises, it intensifies the energy transfer, promoting stronger convective current, reduced momentum boundary layer thickness also allows for more efficient fluid movement which lead to more pronounced flow velocity. More so increase in Temperature profile occurred as well, due to effect of heat transfer mechanisms that is, as the radiation increases it contributes to higher energy absorption within the fluid.

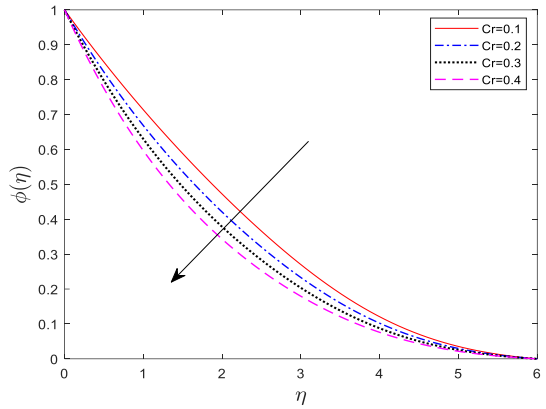

Figure 18: Effect of chemical reaction (Cr) on concentration $\varphi(\eta)$

Figure 18 shows the impact of chemical (Cr) reaction on concentration $\varphi(\eta)$ profiles. An increase in chemical reaction is observed to decline the concentration profile due to rapid consumption of reactants and reduced diffusion driving forces.

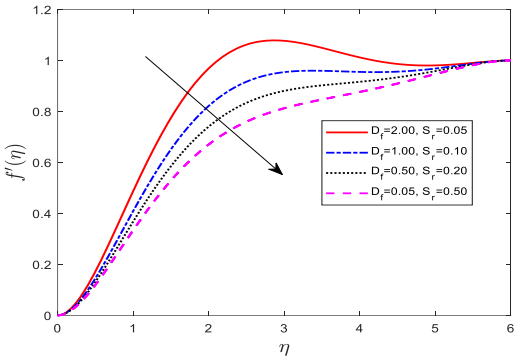

Figure 19: Effect of Dufour number (D_f) and Soret number (S_r) on velocity

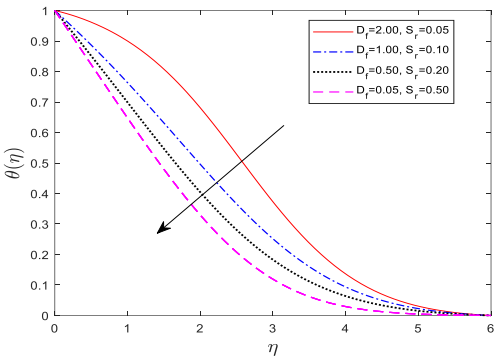

Figure 20: Effect of Dufour number (D_f) and Soret number (S_r) on Temperature$\theta(\eta)$

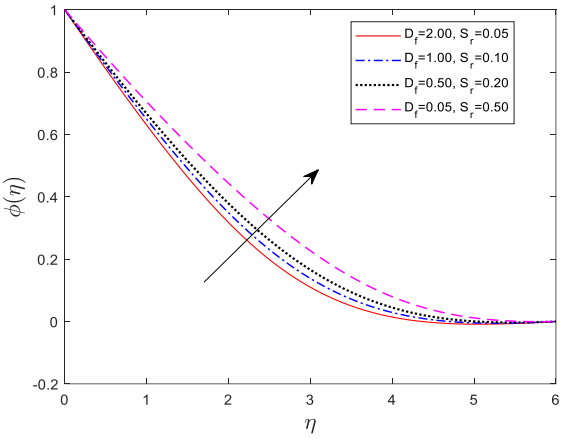

Figure 21: Effect of Dufour number (D_f) and Soret number (S_r) on concentration $\varphi(\eta)$

Figure 19 to 21 shows effect of Dufour number (D_f) and Soret number (S_r) on velocity$f'(\eta)$, temperature$\theta(\eta)$ and concentration $\varphi(\eta)$ respectively. An increase in Dufour number reduced the velocity profile due to heat flux generated by concentration gradients which caused the fluid to be more viscous. Increase in temperature profile occurred because of rise in thermal energy within the fluid. While decrease in concentration profile is observed due to increase in diffusion caused by thermal effects. Additionally, increase in Soret number reduced the velocity profile due to increased resistance and decrease in temperature profile occurred because of heat transfer.

CONCLUSION

The following are the conclusions reached based on the computational analysis of the flow of a couple stress fluid over a vertical plate in the presence of thermal radiation and chemical reaction:

i. Couple stress parameter has dual effect on velocity and increases both temperature and concentration.
ii. Prandtl number reduces both velocity and concentration of the fluid, while Schimdt number and chemical reaction parameter decreases concentration.
iii. Magnetic parameter decreases velocity and advances temperature.

iv. Both temperature buoyancy and mass buoyancy increase fluid velocity, while temperature and concentration are reduced.
v. Radiation parameter increases both velocity and temperature of the fluid.
vi. Dufour number tends to increase velocity and temperature while it decreases the concentration.
vii. Soret number causes a reduction in velocity and temperature while the fluid concentration is increased.

REFERENCES

Ahmed, S., Bég, O. A. and Ghosh, S. K. A. (2014). Couple stress fluid modeling on free convection oscillatory hydromagnetic flow in an inclined rotating channel, *Ain Shams Engineering Journal*, 5:1249-1265.

Ali, F., Sheikh, N. A., Khan, I. and Saqib, M. (2017). Magnetic field effect on blood f low of Casson fluid in axisymmetric cylindrical tube: a fractional model, *J Magn Magn Mater.*, 423:327-336. https://doi.org/10.1016/j.jmmm.2016. 09.125.

Aparna, P. and Ramana, M. J. V. (2008). Oscillatory flow of an incompressible couple stress fluid past a permeable sphere, *Proceedings of 53rd Congress ISTAM, Osmania University, India*, 6:164-173.

Aparna, P., Ramana, M. J. V. and Sreelatha, K. (2007). Uniform flow of an incompressible couple stress fluid past a permeable sphere, *International Electronic Engineering Mathematical Society*, 8:1-10.

Awad, F., Haroun, N. A. H., Sibanda, P., Khumalo, M. (2016). On couple stress effects on unsteady nanofluid flow over stretching surfaces with vanishing nanoparticle flux at the wall, *Journal Applied Fluid Mechanics*, 9:1937 44. https://doi.org/10.18869/acadpub.jafm.68.235.24940.

Bég, A. O., Bhargava, R. and Rashidi, M. M. (2011). *Numerical Simulation in Micropolar Fluid Dynamics*, Saarbrücken: Lap Lambert Academic Publishing GmbH KG.

Bhatti, M. M., Zeeshan, A., Ellahi, R. and Shit, G. C. (2018). Mathematical modeling of heat and mass transfer effects on MHD peristaltic propulsion of two-phase f low through a Darcy-Brinkman-Forchheimer Porous medium, *Advanced Powder Technol.*, 29:1189-1197. https://doi.org/10.1016/j.apt.2018.02.010.

Dawar, A., Shah, Z., Khan, W., Idrees, M. and Islam, S. (2019). Unsteady squeezing flow of magnetohydrodynamic carbon nanotube nanofluid in rotating channels with entropy generation and viscous dissipation, *Adv Mech Eng.*, 11:1-18. https://doi.org/10.1177/1687814018823100.

Ellahi, R., Zeeshan, A., Shehzad, N. and Alamri, S. Z. (2018). Structural impact of Kerosene-Al2O3 nanoliquid on MHD Poiseuille flow with variable thermal conductivity: application of cooling process, *J. Mol. Liquids*, 264:607-615. https://doi.org/10.1016/j.molliq.2018.05.103.

Eringen, A. C. (1966). Theory of micropolar fluids, *J Math Mech.*, 16:1–18. https://doi.org/10.1512/iumj.1967.16.16001.

Farroq, H., Ellahi, R., Zeeshan, A. and Vafai, K. (2018). Modelling study on heated couple stress fluid peristaltically conveying gold nanoparticles through coaxial tubes: a remedy for gland tumors and arthritis, *Journal of Molecular Liquids*, 268:149-155.

Hassan, A. R., Salawu, S. O. and Disu, A. B. (2020). The variable viscosity effects on hydromagnetic couple stress heat generating porous fluid flow with convective wall cooling, *Scientific African*, 9:e00495

Hayat, T., Awais, M., Safdar, A. and Hendi, A. A. (2012). Unsteady three dimensional f low of couple stress fluid over a stretching surface with chemical reaction, *Nonlin. Analy. Mod. Cont.*, 17:47-59. https://doi.org/10.15388/NA.17.1.14077

Hayat, T., Iqbal, R., Tanveer, A. and Alsaed, A. (2016). Soret and Dufour effects in MHD peristalsis of pseudoplastic nanofluid with chemical reaction, *J Mol Liq.*, 220:693-706. https://doi.org/10.1016/j.molliq.2016.04.123.24.

Hayat, T., Mustafa, M., Iqbal, Z. and Alsaedi, A. (2013). Stagnation-point flow of couple stress fluid with melting heat transfer, *Appl Math Mech*, 34:167-176. https://doi.org/10.1007/s10483-013-1661-97.

Khan, A., Shah, Z., Islam, S., Dawar, A., Bonyah, E., Ullah, H. and Khan, A. (2018). Darcy-Forchheimer flow of MHD CNTs nanofluid radiative thermal behaviour and convective non uniform heat source/sink in the rotating frame with microstructure and inertial characteristics, *AIP Adv.*, 8:125024. https://doi.org/10.1063/1.5066223.31.

Khan, N. A., Aziz, S. and Khan, N. A. (2014). Numerical simulation for the unsteady MHD flow and heat transfer of couple stress fluid over a rotating disk, *PLoS ONE*, 9:e95423. https://doi.org/10.1371/journal.pone.0095423.

Kumam, P., Shah, Z., Dawar, A., Rasheed, H. U. and Islam, S. (2019). Entropy Generation in MHD radiative flow of CNTs casson nanofluid in rotating channels with heat source/sink, *Math Problems Eng.*, 2019:9158093. https://doi.org/10.1155/2019/9158093.

Kumar, K. A., Reddy, J. V., Sugunamma, V. and Sandeep, N. (2019). Simultaneous solutions for MHD flow of williamson fluid over a curved sheet with nonuniform heat source/sink, *Heat Transfer Res.*, 50:581–603. https://doi.org/10.1615/HeatTransRes.2018025939.

Lin, Y., Zheng, L., Zhang, X. and Chen, G. (2015). MHD pseudo-plastic nanofluids unsteady flow and heat transfer in a finite thin film over stretching sheet with internal heat generation, *International Journal of Heat and Mass Transfer*, 84:903-911. https://doi.org/10.1016/j.ijheatmasstransfer.2015.01.099.25.

Ramalakshmi, K. and Shukla, P. (2021). Creeping flow of couple stress fluid past a fluid sphere with a solid core, *ZAMM*, 101:e202000115.

Ramesh, K. and Devakar, M. (2015). The influence of heat transfers on peristaltic transport of MHD second grade fluid through porous medium in a vertical asymmetric channel, *J Appl Fluid Mech.* 8:351-365. https://doi.org/10.18869/acadpub.jafm.67.222.23471.26.

Ramkissoon, H. (1978). Drag in couple stress fluids, *ZAMP-Journal of Applied Mathematics and Physics*, 29:341-346.

Ramzan, M., Farooq, M., Alsaedi, A. and Hayat, T. (2013). MHD three-dimensional flow of couple stress fluid with Newtonian heating, *Eur. Phys. J. Plus*, 128:49-56. https://doi.org/10.1140/epjp/i2013-13049.

Reddy, M. G. and Reddy, K. V. (2015). Influence of Joule heating on MHD peristaltic f low of a nanofluid with compliant walls, *Process Eng.*, 127:1002-1009. https://doi.org/10.1016/j.proeng.2015.11.449.

Rudolf, A. T., Baumjohann, W. and Balogh, A. (2014). The strongest magnetic fields in the universe: how strong can they become? *Front Phys.*, 2:59. https://doi.org/10.3389/fphy.2014.0005923.

Shah, Z., Dawar, A., Alzahrani, E. O., Kumam, P., Khan, A. and Islam, S. (2019b). Hall effect on couple stress 3D nanofluid flow over an exponentially stretched surface with Cattaneo Christov Heat Flux Mode, *IEEE Access.*, 7: 64844–55. https://doi.org/10.1109/ACCESS.2019.2916162

Shah, Z., Dawar, A., Kumam, P., Khan, W. and Islam, S. (2019a). Impact of nonlinear thermal radiation on MHD nanofluid thin film flow over a horizontally rotating disk, *Appl. Sci.*, 9:153-163. https://doi.org/10.3390/app9081533.

Sreenadh, S., Kishore, S. N., Srinivas, A. N. S. and Reddy, R. H. (2011), MHD free convection f low of couple stress fluid in a vertical porous layer, *Adv. Appl. Sci. Res.*, 2:215-222.

Srinivasacharya, D. and Kaladhar, K. (2012). Mixed convection flow of couple stress fluid in a non-darcy porous medium with Soret and Dufour effects, *Journal of Applied Science and Engineering*, 15:415-22.

Stokes, V. K. (1966). Couple stresses in fluids, *Physics Fluids*, 9:1709-1715.

Temple, R. C., Mihai, A. P., Arena, D. A. and Marrows, C. H. (2015). Ensemble magnetic behavior of interacting CoFe nanoparticles, *Front Phys.*, 3:52. https://doi.org/10.3389/fphy.2015.00052.

Turkyilmazoglu, M. (2014). Exact solutions for two-dimensional laminar flow over a continuously stretching or shrinking sheet in an electrically conducting quiescent couple stress fluid, *International Journal of Heat and Mass Transfer*, 72:1-8. https://doi.org/10.1016/j.ijheatmasstransfer.2014.01.0098.

Uddin, Z. and Kumar, M. (2013). Hall and ion-slip effect on MHD boundary layer f low of a micro polar fluid past a wedge, *Sci. Iran*, 20:467-476. https://doi.org/10.1016/j.scient.2013.02.01330.